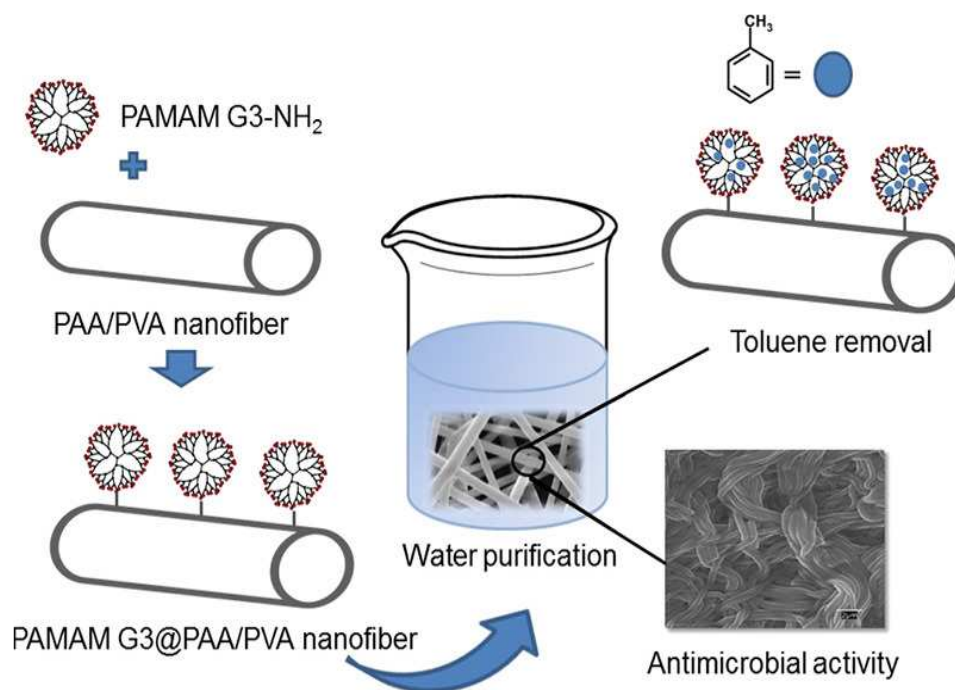


# Dendrimer-functionalized electrospun nanofibres as dual-action water treatment membranes

Please, cite as follows:

Georgiana Amariei, Javier Santiago-Morales, Karina Boltes, Pedro Letón, Isabel Iriepa, Ignacio Moraleda, Amadeo R. Fernández-Alba, Roberto Rosal, Dendrimer-functionalized electrospun nanofibres as dual-action water treatment membranes, *Science of The Total Environment*, Volume 601–602, 1 December 2017, Pages 732-740, ISSN 0048-9697, <https://doi.org/10.1016/j.scitotenv.2017.05.243>.



# Dendrimer-functionalized electrospun nanofibres as dual-action water treatment membranes

Georgiana Amariei<sup>1</sup>, Javier Santiago-Morales<sup>1</sup>, Karina Boltes<sup>1</sup>, Pedro Letón<sup>1</sup>, Isabel Iriepa<sup>2</sup>, Ignacio Moraleda<sup>2</sup>, Amadeo R. Fernández-Alba<sup>3</sup>, Roberto Rosal<sup>1,\*</sup>

<sup>1</sup> Department of Chemical Engineering, University of Alcalá, E-28871 Alcalá de Henares, Madrid, Spain

<sup>2</sup> Department of Organic Chemistry and Inorganic Chemistry, School of Biology, Environmental Sciences and Chemistry, University of Alcalá, E-28871 Alcalá de Henares, Madrid, Spain

<sup>3</sup> Department of Analytical Chemistry, Agrifood Campus of International Excellence (ceiA3), European Union Reference Laboratory for Pesticide Residues in Fruit & Vegetables, University of Almeria, E-04010 Almería, Spain

\* Corresponding author: roberto.rosal@uah.es

## Abstract

This work reports the preparation of composite electrospun membranes combining antimicrobial action with the capacity of retaining low-molecular weight non-polar pollutants. The membranes were electrospun blends of polyvinyl alcohol (PVA) and poly(acrylic acid) (PAA) stabilized using heat curing. The membranes were functionalized by grafting amino-terminated poly(amidoamine) (PAMAM) G3 dendrimers. The antimicrobial effect was assessed using strains of *Escherichia coli* and *Staphylococcus aureus* by tracking their capacity to form new colonies and their metabolic impairment upon contact with membranes. The antimicrobial activity was particularly high to the gram-positive bacterium *S. aureus* with a 3-log reduction in their capacity to colonize dendrimer-functionalized membranes with respect to neat PVA/PAA fibers. The effect to gram-positive bacteria was attributed to the interaction of dendrimers with the negatively charged bacterial membranes and resulted in membranes essentially free of bacterial colonization after 20 h in contact with cultures at 36 °C. The adsorption of toluene on PAA/PVA fibers and on dendrimer-functionalized membranes was assayed using toluene over a broad concentration range. The host-guest encapsulation of toluene inside dendrimer molecules was computed through docking studies, which allowed calculating a maximum capacity of 14 molecules of toluene per molecule of PAMAM G3. The theoretical prediction was in good agreement with the experimental capacity at the higher concentrations assayed.

**Keywords:** Dendrimers; Molecular docking; Electrospinning; Poly(acrylic acid); Poly(vinyl alcohol); Antimicrobial membranes

## 1. Introduction

Dendrimers are hyper-branched monodispersed polymers that consist of a central core, from which radially branched monomers, referred to as dendrons, grow in successive layers, called generations (G) (Vögtle *et al.*, 2009). Their globular and highly symmetric structure exposes a large number of surface end-groups, a property that makes them attractive in terms of functionalization chemistry. Additionally, they possess relatively large internal cavities allowing remarkable core encapsulation capacity and acting as solubility enhancers (Malkoch *et al.*, 2012). As a consequence of these properties, dendrimers have been used and tested for a wide range of applications such as catalytic, sensing, environmental and biomedical uses (Astruc *et al.*, 2010; Astruc and Chardac, 2001; Khin *et al.*, 2012; Svenson and Tomalia, 2005).

Supported dendrimers have been proposed for different interphase applications. Poly(amidoamine) (PAMAM) dendrimers have been used to create supported palladium or platinum catalysts (Bukowska *et al.*, 2015;

Ledesma-García *et al.*, 2008). A similar approach led to gold nanoparticle heterogeneous catalysts using polymer-supported poly(propyleneimine)-G2 dendrimers and the dendrimer encapsulation of ruthenium nanoparticles (Antonels *et al.*, 2016; Murugan and Rangasamy, 2010). Surface-immobilized dendrimers have also been proposed for different kinds of dendritic sensors (Altintas *et al.*, 2012; Satija *et al.*, 2014; Valdés *et al.*, 2016). Concerning biomedical uses, dendrimer-based active membranes have been designed to create substrates with increased contact between cells and scaffold (Zhang *et al.*, 2016). Electrospun cellulose acetate nanofibres were modified with PAMAM G5 dendrimers loaded with folic acid for the capture of cancer cells overexpressing folic acid receptors (Zhao *et al.*, 2014). In an environmental application, metalloporphyrin-PAMAM dendrimers supported on mesoporous MCM-41 allowed the extraction of nitrosamine from water (Sanagi *et al.*, 2015). In another approach, cellulosic membranes with poly(propyleneimine) dendrimers were used for retaining heavy metals (Algarra *et al.*, 2014).

Electrospinning is the only general technique available for the production of nanopolymeric fibers. In it, a jet of fluid is extruded out of a capillary and subjected to a high potential difference with respect to a grounded collector electrode. As a result of the electrostatic interaction the jet accelerates in a whipping-like motion and the solvent evaporates yielding a solid fiber collected forming an ordered array or a disordered nonwoven matrix (Bhattacharjee and Rutledge, 2011). Electrospun fibers find a wide range of applications in many technological areas thanks to their high surface-to-volume ratio and the possibility of producing tailored fibers via chemical modification or the incorporation of non-spinnable materials (Greiner and Wendorff, 2007). The fabrication of bioactive fibers is one the most promising areas, which include antimicrobial materials, scaffolds for tissue engineering, fibers for controlled drug release or active wound dressings among other applications (Quirós et al., 2016). The main environmental application of nanofibrous membranes is the production of filtration membranes with minimal pressure drop and the possibility of incorporating different functionalities (Thavasi et al., 2008).

Poly(acrylic acid) (PAA) and polyvinyl alcohol (PVA) are water-soluble polymers that can be processed without the use of organic solvents. In particular, the electrospinning of PAA or PVA solutions can produce ultrafine materials that cannot be obtained by conventional spinning techniques. Electrospun ultrafine fibers of PAA and PVA have a number of potential applications in filtration and biomedical engineering in view of their high surface area, chemical tunability and biocompatibility (Kim et al., 2005; Zhang et al., 2005). PAA and PVA can be crosslinked rendering materials with different swelling behavior depending on the annealing time and temperature, the molecular weight of polymers and their mixture ratio (Kumeta et al., 2003). Besides, the antimicrobial activity of poly(acrylic acid) based polymers has been recently documented (Gratzl et al., 2015; Santiago-Morales et al., 2016).

Non-polar light aromatics, notably benzene, toluene, ethylbenzene and xylenes, jointly referred to as BTEX, are widely used compounds, which, due to their mobility and solubility, can enter the soil and groundwater compartments causing serious pollution problems. BTEX reach the environment through the emissions from motor vehicles, the leaking of storage tanks, and the use of a number of consumer goods, including paints, cosmetics and pharmaceutical products. Concerns have recently arisen regarding the drinking-water contamination due to BTEX and other chemicals associated to hydraulic fracturing and horizontal drilling practices (Gross et al., 2013). According to the World Health Organization (WHO), the guideline value for benzene, toluene, ethylbenzene, and xylene in drinking water are 0.01, 0.7, 0.3 and 0.5 mg/L, respectively. However, concentrations of

toluene in water one order of magnitude lower can give bad odor and taste (WHO, 2011).

In this work we prepared active electrospun membranes combining antimicrobial action with the capacity of retaining low-molecular weight non-polar pollutants from aqueous solution. The antimicrobial action has been tested with strains of *Escherichia coli* and *Staphylococcus aureus* by studying their capacity to form new colonies and the impairment induced in bacterial cells. The removal of aqueous pollutants, was assayed using toluene in a broad concentration range to gain insight into the interaction between small hydrophobic aromatic entities and dendrimers. For it, we investigated the host-guest association through docking studies of toluene and PAMAM-G3 dendrimers.

## 2. Experimental

### 2.1. Materials

Poly(vinyl alcohol) (PVA, MW 89–98 kDa, > 99% hydrolyzed) and poly(acrylic acid) (PAA, MW 450 kDa) from Sigma-Aldrich were used for preparing the polymeric fibers. Ultrapure water (Millipore Milli-Q System) with a resistivity of at least 18 M $\Omega$  cm was employed for dissolving PVA and PAA. *N,N*-dicyclohexylcarbodiimide (DCC, MW 206.33, 99%) was obtained from Sigma-Aldrich. PAMAM dendrimer generation 3 (PAMAM G3-NH<sub>2</sub>), 20 wt% solution in methanol and 9.43 wt% solution in water, were purchased from Sigma Aldrich and Dendritech®. Inc. (Midland, MI), respectively. Dimethyl formamide (DMF, 99%) and absolute ethanol were acquired from Sigma-Aldrich. Fluorescein diacetate (FDA, 99.9%) and dimethyl sulfoxide (DMSO, 99.9%) were also obtained from Sigma-Aldrich. The components of culture media and buffers were purchased to Conda-Pronadisa (Spain).

### 2.2. Membrane preparation

The production of PAA/PVA fibers was performed by electrospinning. Briefly, the spinning solution was prepared using a polymeric solution mixture composed of 8 wt% PAA and 15 wt% PVA in ultrapure water with a final PAA/PVA weight ratio of 35:65. The solution was stirred for 2 h, at 25 °C and degassed prior to electrospinning. The solution was set into a 5 mL syringe fitted with a 23-gauge stainless steel blunt needle and electrospun using the following parameters: voltage, 23 kV; distance from the needle tip to collector, 23 cm and flow rate 0.8 mL/h. A drum collector (PDrC-3000, Yflow, Spain) rotating at 100 rpm was used. The whole electrospinning apparatus was enclosed in a chamber at 40% RH and 25 °C. The electrospun fibers were collected on aluminum foil and dried at 50 °C for 24 h. After that, the nanofibres were crosslinked by heating at 140 °C for 30 min. The crosslinked fibers were washed with distilled water and dried under vacuum (50 °C, 24 h) prior to functionalization.

The functionalization of PAA/PVA membranes was performed by grafting G3 NH<sub>2</sub>-terminated PAMAM dendrimers onto fibers via amide formation with their surface carboxyl groups. DCC was used as a coupling agent for the reaction as indicated elsewhere (Tsubokawa et al., 1995). In order to tune the amount of PAMAM G3 grafted on PAA/PVA fibers, two solvents, DMF and ethanol, and two PAMAM G3 solutions, in methanol and water, were used as indicated in Table 1. For a typical grafting reaction, a mixture of 8.0 mL of solvent, 41.2 mg of DCC and 1  $\mu$ L of PAMAM G3 in methanol or 1.83  $\mu$ L of PAMAM G3 in water, equivalent to 0.2 mol G3/mol COOH, was stirred overnight at 25 °C to ensure homogeneity. Previously dried and accurately weighed PAA/PVA membranes were immersed into the PAMAM/DCC/solvent mixture solution and orbitally shaken at 100 rpm for 24 h. After the amide formation reaction, the membranes were removed, rinsed with the solvent, DMF or ethanol, washed with deionized water for kept in water bath for 16 h in order to remove the unattached PAMAM molecules and residual reagents. Finally, the membranes were dried in vacuum (10 kPa) at 100 °C for 24 h ensuring constant weight.

### 2.3. Membrane characterization

The surface morphology of membranes was studied by field emission scanning electron microscopy (SEM) using a DSM-950 (Zeiss, Oberkochen, Germany) apparatus operating at 25 kV. Before observation, the samples were sputter-coated with gold. Atomic force microscopy imaging (AFM) was performed using a Bruker multimode Nanoscope III A. Attenuated Total Reflectance Fourier Transform Infrared (ATR-FTIR) spectra were obtained using a Thermo-Scientific Nicolet iS10 apparatus equipped with a Smart iTR-Diamond ATR module. The grafting of G3 dendrimers onto the fiber surface was also assessed by IR spectroscopy using a Vector22, Bruker instrument. The surface charge of membranes was measured as  $\zeta$ -potential using dynamic light scattering in a Zetasizer NanoZS equipment equipped with a ZEN 1020 Cell (Malvern Instruments, UK). For it, a small section of the membrane was glued to the sample holder and inserted into a disposable 10 mm plastic cuvette containing 10 mM KCl, pH 7.0 with of 0.5 wt% PAA (450 kDa) as tracer. Measurements were conducted at 25 °C at six different distances from membrane surface.

Total Organic Carbon (TOC) was measured as NPOC (Non-Purgeable Organic Carbon) using a Shimadzu, TOC-VCSH) analyzer. The nitrogen content of the samples was determined by elemental analysis using a LECO CHNS/O-932 equipment, which allowed calculating the amount of dendrimer grafted per unit mass of PAA/PVA membrane. The amount of carboxyl groups per unit mass of neat PAA/PVA membrane was measured determined by titration of carboxyl groups. Membrane samples were weighed and protonated using 0.1 M HCl for 24 h, washed with deionized water to remove excess HCl and immersed in 0.1 M NaOH for 24 h. The resulting NaOH solution was titrated with 0.1 M HCl and the result expressed as moles of carboxyl groups per unit mass of dry membrane. The experiments were carried out under nitrogen atmosphere.

### 2.4. Antimicrobial activity assessment

Neat PAA/PVA and G3@PAA/PVA functionalized materials were studied for testing their antibacterial activity against the gram-positive *S. aureus* (CETC 240) and the gram-negative *E. coli* (CETC 516) bacterial strains. The microorganisms were reactivated using nutrient broth (NB, 10 g L<sup>-1</sup> peptone, 5 g L<sup>-1</sup> sodium chloride, 5 g L<sup>-1</sup> meat extract and, for solid media, 15 g L<sup>-1</sup> powder agar, pH 7.0  $\pm$  0.1), at 30 °C under agitation (150 rpm) and routinely tracked by measuring optical density (OD) at 600 nm. Dry functionalized PAA/PVA membranes (weighed pieces of approx. 6 mg) were placed into wells of sterile 24-well plate. Neat PAA/PVA membranes were used as negative control. A culture of 10<sup>6</sup> cell/mL was prepared by standard serial dilution and 2.4 mL of bacterial suspension was added in the 24 well-plate followed by incubation at 36 °C for 20 h. After the prescribed exposure time, the membranes were removed from the culture media, transferred to clean 24-well plates with phosphate-buffered saline (PBS) and incubated under agitation for 10 min at 5 °C, in order to remove non-adhered cells at a temperature low enough to avoid microbial growth. Next, the cells adhered on membrane surface were recovered by replacing PBS by 2 mL/well SCDLP (Soybean casein digest broth with lecithin and polyoxyethylene sorbitan monooleate) broth according to ISO 22196 and re-incubating for 30 min at 5 °C, under agitation. Finally, the antibacterial activity was assessed by plate counting of viable cells and by determining cell viability as indicated below.

**Table 1.** Materials prepared in this investigation

Membrane	Dendrimer used	Functionalization solvent	G3 content ( $\mu$ mol G3/g membrane)	Surface $\zeta$ -potential (mV)
PAA/PVA	-		-	-35.2 $\pm$ 0.2
G3[1]@PAA/PVA	G3 9.43 % in H <sub>2</sub> O	DMF	6.49 $\pm$ 0.16	-4.4 $\pm$ 0.5
G3[2]@PAA/PVA	G3 20 % in Methanol	DMF	2.63 $\pm$ 0.17	-8.6 $\pm$ 1.2
G3[3]@PAA/PVA	G3 9.43 % in H <sub>2</sub> O	Ethanol	1.10 $\pm$ 0.35	-11.7 $\pm$ 2.4
G3[4]@PAA/PVA	G3 20 % in Methanol	Ethanol	0.80 $\pm$ 0.04	-15.6 $\pm$ 0.4

The supernatant liquid after 20 h exposure and the suspension resulting from cell detachment were serially diluted in PBS. From these dilutions, 4 mini-spots of 10  $\mu$ L per dilution were dispensed in Petri dishes containing standard rich agar-medium (ISO 22196). After inoculation, the plates were incubated at 36  $^{\circ}$ C and the colonies were counted after 16 h. For the Colony Forming Unit (CFU) calculations at least 3 replicates of at least two serial dilutions were computed for each sample. The bacterial viability was measured using the fluorescein diacetate (FDA) staining method as described elsewhere (Quiros et al., 2015). In it, non-fluorescent FDA is transformed by the active esterases of fully functional cells into the green-fluorescent compound fluorescein. Briefly, the samples were analysed in 96-well microplate by adding 195  $\mu$ L test aliquot and 5  $\mu$ L of FDA (0.02% w/w in DMSO) to each well. Then the plates were incubated for 5 min at 25  $^{\circ}$ C and the fluorescence recorded every 5 min for 30 min (using a fluorometer (ThermoScientific™ FL, Ascent) with excitation at 485 nm and emission at 528 nm. All experiments indicated before were performed replicated until obtaining correct accuracy and precision.

SEM and confocal micrographs of membranes colonized by *E. coli* and *S. aureus* were also taken after inoculation with  $10^6$  cells/mL and incubation in NB medium at 36  $^{\circ}$ C for  $20 \pm 1$  h. For SEM images, membranes were cleaned with distilled water, fixed and dehydrated with ethanol and acetone. SEM micrographs were obtained in a ZEISS DSM-950 instrument operating at 25 kV. Cell viability and membrane damage were tracked by means of the Live/Dead BacLight Bacterial Viability Kit (Molecular Probes, Invitrogen, Carlsbad, CA, USA). This combination of two nucleic acid stains makes all cells exhibit green fluorescence (SYTO 9), whereas bacterial cells with compromised membrane integrity display red fluorescence (propidium iodide, PI). Membrane specimens and supernatant liquid in contact with them were stained with 10 mL BacLight stain (a mixture of SYTO 9 and PI in DMSO) according to the manufacturer's recommendations following 15 min incubation in the dark at room temperature.

## 2.5. Toluene removal from water

The ability of PAMAM G3-functionalized membranes to remove small non-polar molecules from water was evaluated using toluene solutions. Neat and PAMAM G3-functionalized electrospun membranes were immersed in an aqueous solution of toluene and shaken for 24 h at room temperature. Different ratios of membrane to toluene were tested with toluene concentrations ranging from 1 to 200 mg/L.

Toluene concentration was determined by head-space-gas chromatography-simple quadrupole-mass spectrometry analysis. An Agilent 7697A head-space sampler coupled to an Agilent 7890A GC system, and an Agilent 5975C inert XL MSD were used for the

analyses. Data acquisition were developed using Agilent Chemstation v.02 software. Headspace operating conditions were as follows: oven temperature, 90  $^{\circ}$ C; sample loop/valve temperature, 100  $^{\circ}$ C; transfer line temperature, 110  $^{\circ}$ C; pressurization equilibration time, 0.5 min; vial equilibration time, 30 min; inject time, 0.25 min; and GC cycle time, 40 min. The samples were injected using a split-splitless inlet in split mode with split ratio of 15:1 at a helium flow of 17.3 mL/min, through a deactivated tapered borosilicate with a glass wool frit, from Agilent. The injection volume was 1 mL. The injector temperature was kept at 250  $^{\circ}$ C. An Ultra Inert GC column (Agilent), DB-624 60 m  $\times$  0.25 mm  $\times$  1.4  $\mu$ m, was used to provide analytical separation. The oven temperature program was as follows: 50  $^{\circ}$ C for 5 min, up to 170  $^{\circ}$ C at 6  $^{\circ}$ C/min and hold for 1 min and finally up to 240  $^{\circ}$ C at 40  $^{\circ}$ C/min and maintained for 1 min. The total run time was 28.75 min plus 3 min for equilibrating the column at 50  $^{\circ}$ C. The instrument worked at constant pressure (19.9 psi). Helium (99.999% purity) was used as the carrier gas. Both the transfer line and the ion source, operated in electron ionization, were maintained at 230  $^{\circ}$ C. Quadrupole analyzer temperature was 150  $^{\circ}$ C. The solvent delay was 4.6 min. The mass spectrometer was used selected ion monitoring (SIM) mode after identification of the relevant peaks in full scan mode (35 to 100 amu). The appropriate ions selected for toluene were  $m/z$ : 51, 65, 91 and 92. For the higher concentrations, toluene concentration was determined by UV absorbance at 261 nm recorded by means of a Shimadzu SPD-6AV spectrophotometer.

## 2.6. Computational procedure

Docking calculations were performed using the program Autodock Vina (Trott and Olson, 2010). AutoDockTools (ADT; version 1.5.4) was used to add hydrogens and partial charges to dendrimer and ligand using Gasteiger charges. Flexible torsions in the ligand were assigned with the AutoTors module, and the acyclic dihedral angles were allowed to rotate freely. Vina uses rectangular boxes for the binding site. Therefore, the box center was defined and the docking box was displayed using ADT. The initial dendrimer structure was obtained from Maingi et al. (2012), using the structure with the terminal amine groups are protonated to mimic PAMAM dendrimer at neutral pH conditions. The docking procedure was applied to the whole dendrimer, without imposing the binding site. This process is considered a blind docking. Using the GridBox option, the 3-dimensional parameters for docking the ligand to the dendrimer were determined. The grid center coordinates were  $x = 46.579$ ,  $y = 17.652$ ,  $z = 29.472$  and the size coordinates were  $x = 50$ ,  $y = 46$ ,  $z = 48$  with grid points separated 1  $\text{Å}$ . Default parameters were used except num\_modes, which was set to 40. The center of the grid box was chosen in such a way that the search space for toluene was limited to the inner region of the dendrimer. Toluene was assembled within Discovery Studio,

version 2.1, software package, using standard bond lengths and bond angles. With the CHARMM force field (Brooks et al., 1983) and partial atomic charges, the molecular geometry of toluene was energy-minimized using the adopted-based Newton-Raphson algorithm. Structures were considered fully optimized when the energy changes between iterations were  $< 0.01$  kcal/mol (Morreale et al., 2002). Toluene was docked 50 times into the dendrimer and the docking results generated were directly loaded into Discovery Studio, version 2.1 for their analysis. The best scoring docked conformation was selected for each case.

### 3. Results and Discussion

#### 3.1. Functionalized nanofibres

PAA/PAA electrospun membranes were stabilized by crosslinking esterification for 30 min at 140 °C, after which they were kept in water until constant weight. The amount of polymer released during 24 h membrane conditioning was  $9.7 \pm 0.2$  mg/g of membrane measured as NPOC, which decreased to  $1.6 \pm 0.1$  mg/g of membrane during a subsequent 24 h immersion in water, after which they underwent negligible weight change. The membranes used in this work were water preconditioned for 48 h. The quantification of free carboxyl groups measured by titration as indicated before yielded  $8.0 \pm 0.3$  mmol COOH/g of membrane. Neat PAA/PVA membranes were used as base material for dendrimer functionalization, which was performed using two solvents (DMF and ethanol) and two different PAMAM G3 solutions (in water and methanol). The amount of dendrimer grafted per unit mass of membrane is shown in Table 1 for each case and was considerably larger when using DMF as solvent. All membranes listed in Table 1 were used in microbiological tests, while the G3[1]@PAA/PVA membrane, with the largest amount of grafted dendrimer, was assayed for toluene removal from water.

The different yield in amide bond formation can be rationalized from the presence of nucleophiles in the reaction mixture. Carboxyl groups in PAA/PVA membranes reacted with the carbodiimide coupling agent DCC to produce the intermediate O-acylisourea. In the presence of amines, the carbocation intermediate (an electrophile) gives rise to an amide bond, but other nucleophiles in solution such as ethanol can react with it reducing the amount of amide bond formation (Montalbetti and Falque, 2005). This explains why in the presence of a large excess of ethanol (G3[3]@PAA/PVA and G3[4]@PAA/PVA membranes) the extent of dendrimer grafting was lower in comparison with the membranes prepared in the aprotic solvent DMF. A lower degree of amide formation was also observed in materials produced from G3 in methanol compared to water, which can also be attributed to the reaction of methanol with the intermediate O-acylisourea. A typical by-product of the carbodiimide reaction with carboxyl groups is a N-

acylurea, which is stable in aqueous media, and lowers the yield of amide formation. It was reported that N-acylurea was formed only when an excess of carbodiimide is present, so we used an equimolar amount of DCC with respect to the carboxyl groups in PAA/PVA membranes (Valeur and Bradley, 2009). The dicyclohexylurea formed was washed out of functionalized membranes as demonstrated by the decrease of the total nitrogen content of membranes down to a stable value during washing.

The surface charge of the dendrimer-grafted membranes showed a considerable decrease in the negative values of  $\zeta$ -potential from the  $-35.2 \pm 0.2$  mV of PAA/PVA membranes to the  $-4.4 \pm 0.5$  mV of the specimens with the highest amount of dendrimer incorporated. The reason was the positive surface charge of PAMAM G3 dendrimers at pH 7.0 due to the partial protonation of terminal amino groups (Boas and Heegaard, 2004).

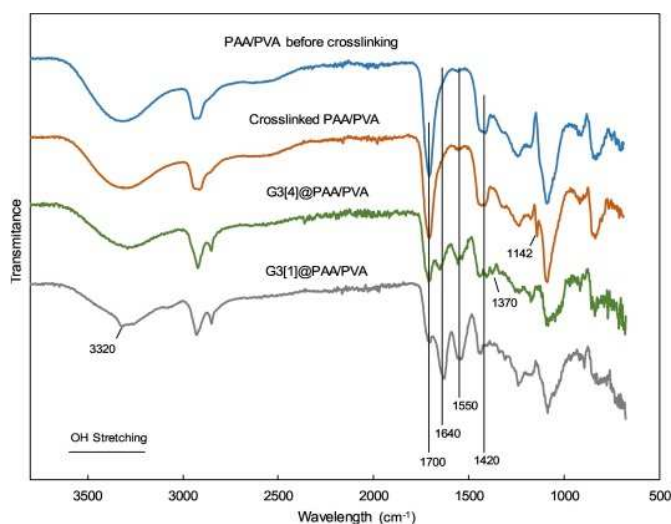


**Figure 1.** ATR- FTIR spectra of PAA/PVA fibers before and after crosslinking and dendrimer-functionalized membranes G3[1]@PAA/PVA and G3[4]@PAA/PVA.

FTIR spectra revealed the major peaks associated with PVA and PAA. The broad O-H stretching band ( $3200\text{--}3600\text{ cm}^{-1}$ ) is the most characteristic feature of alcohols and corresponds to the stretching vibration of hydroxyl group with strong hydrogen bonding (Nouh and Bahareth, 2013). The C-H alkyl stretching band ( $2850\text{--}3000\text{ cm}^{-1}$ ) was also clear together with the absorption peak  $1142\text{ cm}^{-1}$ , which can be attributed to the C-O stretching in the crystalline domains of PVA (Mansur et al., 2004). The characteristic carboxyl stretching frequency of PAA is observed at  $1700\text{ cm}^{-1}$ , while the symmetric and antisymmetric stretching frequencies of the carboxylate ion ( $\text{COO}^-$ ) appeared at  $1420$  and  $1560\text{ cm}^{-1}$  (Kirwan et al., 2003). After thermal crosslinking, the OH and C=O stretching bands decreased due to the formation of anhydride, ketone and ester groups (Jin and Hsieh, 2005) (Arndt et al., 1999). These changes were accompanied by a weight loss of  $\sim 5$  wt%, which can be attributed to the release of residual monomers and  $\text{CO}_2$  evolution from

anhydride decarboxylation (Dubinsky et al., 2005). Additional details on the thermal crosslinking process can be found elsewhere (Santiago-Morales et al., 2016).

In functionalized fibers, the signals of primary amine N-H stretch at  $3320\text{ cm}^{-1}$ , N-H bending at  $1550\text{ cm}^{-1}$  and the C=O stretching band from the internal amides at  $1640\text{ cm}^{-1}$  were clearly recognizable. At pH 7 the surface primary amines of PAMAM dendrimers were partly charged as their pKa is 6.85 (Tomalia et al., 1990). N-H stretch appeared shifted to higher wavelength numbers as a shoulder in the broad O-H band in quaternary ammonium dendrimer salts (Charles et al., 2012). The increase in the alkyl stretching signal with a clear separation between  $\text{CH}_2$  asymmetric stretching band at  $2924\text{ cm}^{-1}$  and CH stretching symmetric band at  $2848\text{ cm}^{-1}$  is also evidencing the attachment of dendrimers to PAA/PVA fibers. In addition, the decrease in the carboxyl signals at  $1700\text{ cm}^{-1}$  and  $1420\text{ cm}^{-1}$  indicated the reaction of carboxyl groups. When ethanol was used as a solvent, the reaction with dendrimers yielded acetate groups, the characteristic signal of which, at  $1370\text{ cm}^{-1}$ , was clear in G3[4]@PAA/PVA IR spectrum (Fig. 1). Fig. 2 shows SEM micrographs of freshly electrospun PAA/PVA membranes, after crosslinking (30 min), and after functionalization (and subsequent drying for SEM). Fig. 2a corresponds to a crosslinked PAA/PVA membrane as produced, before water immersion and functionalization. The average fiber diameter, obtained from SEM images was  $301 \pm 28\text{ nm}$  with uniform, straight and well-defined fibers free from beading or other flaws. After functionalization (using DMF or ethanol) and water immersion the membranes kept their fibrous morphology with fiber swelling and occasional merging between adjacent fibers and at their contact points. Fig. 2b and c show micrographs for G3[1]@PAA/PVA membranes at two magnifications.

Representative images for the rest of membranes are presented in Fig. S1 (Supplementary material) showing in all cases, membranes with fiber-based morphology and considerable fiber merging. No significant differences were found in any case concerning fiber

aspect or diameter among functionalization treatments. Fig. S2 in Supplementary material shows AFM images of a G3[1]@PAA/PVA membrane including a height profile and a 3D view. The AFM images confirmed the topographic characteristics depicted by SEM. The swelling behavior that led to fiber merging was a consequence of the well-known tendency of both PAA and PVA to form hydrogels and has been reported elsewhere (Jin and Hsieh, 2005; Park et al., 2010; Santiago-Morales et al., 2016). The preservation of the fibrous structure is noteworthy and essential for keeping access to the functional groups grafted to fiber surface allowing their application as active membranes in aqueous media.

### 3.2. Antimicrobial activity assessment

The antimicrobial efficiency of dendrimer-functionalized membranes was evaluated using the inhibition of bacterial growth and metabolic cell impairment using the gram-negative *E. coli* and the gram-positive *S. aureus*. Fig. 3a and b shows the reduction in the capacity of forming viable colonies in the culture medium media in contact with membranes during the incubation period of 20 h at  $36\text{ }^\circ\text{C}$ . Both bacterial strains were damaged in their capacity to form new colonies, but the effect was higher to *S. aureus* than to *E. coli*. *S. aureus* decreased the number of CFU up to 99.6% ( $> 2\text{ log}$ ) while the inhibition of *E. coli* amounted to only near 50% with respect to PAA/PVA. It is noteworthy that neat PAA/PVA fibers already display a considerable antimicrobial action before functionalization, particularly for PAA contents  $> 35\text{ wt\%}$  (Santiago-Morales et al., 2016). The capacity of forming colonies for bacteria adhered to the membrane surface was also considerably inhibited for both strains (Fig. 3c). Again, the effect was higher to *S. aureus* (99.9%) than to *E. coli* (88%). Either in the case of liquid culture in contact with membranes or microorganisms detached from them, the effect was higher for dendrimer-loaded membranes, particularly G3[1]@PAA/PVA, the membrane with the highest content of PAMAM G3.

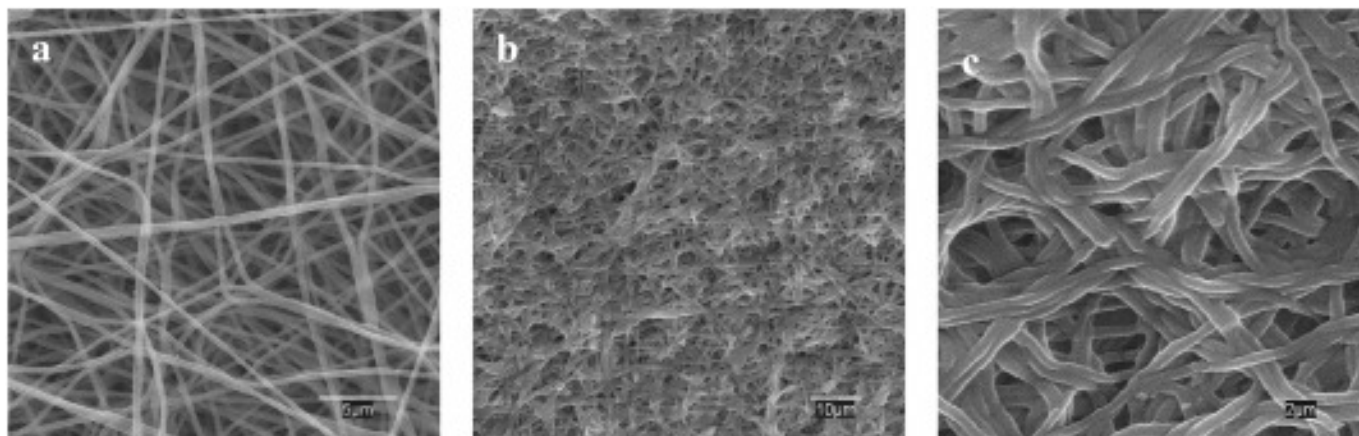


**Figure 2.** SEM micrographs of crosslinked PAA/PVA membranes (a) and G3[1]@PAA/PVA dendrimer-functionalized fibers at two magnifications (b and c).

The damage was also assessed by means of FDA, a stain that tracks the metabolic activity of live cells, which are those with esterases capable of transforming the non-fluorescent FDA into fluorescein. The results are shown in Fig. 3d. The data showed that *S. aureus* was significantly impaired, with a decrease in cell metabolic activity > 95 % for G3[1]@PAA/PVA, with respect to PAA/PVA fibers. The damage to *E. coli* was lower, with a maximum of 45% for the higher dendrimer content. In all cases, the decrease in cell metabolic activity was lower than the inhibition of their capacity to form new colonies. This result is most probably due to the presence of viable but non-culturable (VBNC) bacteria. VBNC bacteria display substantial metabolic activity but fail to replicate in plate count assays. VBNC state is survival strategy commonly adopted by many bacterial strains in response to adverse environmental conditions including the presence of antimicrobials such as disinfectants or chemotherapeutic agents (Ramamurthy et al., 2014).

The effect of PAA/PVA can be attributed to the chelation of the divalent cations stabilizing the outer cell membrane or, in the case of gram-positive bacteria to the destabilization of the peptidoglycan layer. The abstraction of the divalent counter-ions that balance the negative charges of the bacterial cell membrane components would result in a collapse of the cell membrane (Gratzl et al., 2015). The effect on bacterial growth and the appearance of cells with damaged

membrane was revealed by the confocal micrographs shown in Figs. S3 and S4 (SM), which correspond to Live/Dead confocal micrographs of *E. coli* and *S. aureus* from the liquid culture in contact with G3[1]@PAA/PVA and PAA/PVA membranes and to cells on membrane surface. The images show a lower amount of viable cells on dendrimer-loaded membranes, particularly for *S. aureus* as shown in Fig. S4e and g, which correspond to surfaces essentially clean of bacterial proliferation. Certain cells appeared yellowish or orange, which is generally considered a transitional state between viable and damaged cells (Boulos et al., 1999). The differences between both strains can be rationalized in terms of the structure of the outer layers of gram-negative and gram-positive bacteria. In gram-positive bacteria, the outer membrane is a thick peptidoglycan layer but in gram-negative bacteria the peptidoglycan layer lies between plasma membrane and the lipopolysaccharide outer membrane, which in turn is stabilized by repulsive forces due to accumulation of the negative charges bridged by divalent cations. The peptidoglycan layer, although relatively thick, is porous and allows easy access to the internal membrane. The absence of an outer membrane makes gram-positive bacteria more susceptible to the effect of antimicrobials than Gram-negative bacteria (Silhavy et al., 2010). The removal of the stabilizing cations would induce higher cell impairment in *S. aureus* than in *E. coli* (Santiago-Morales et al., 2016).

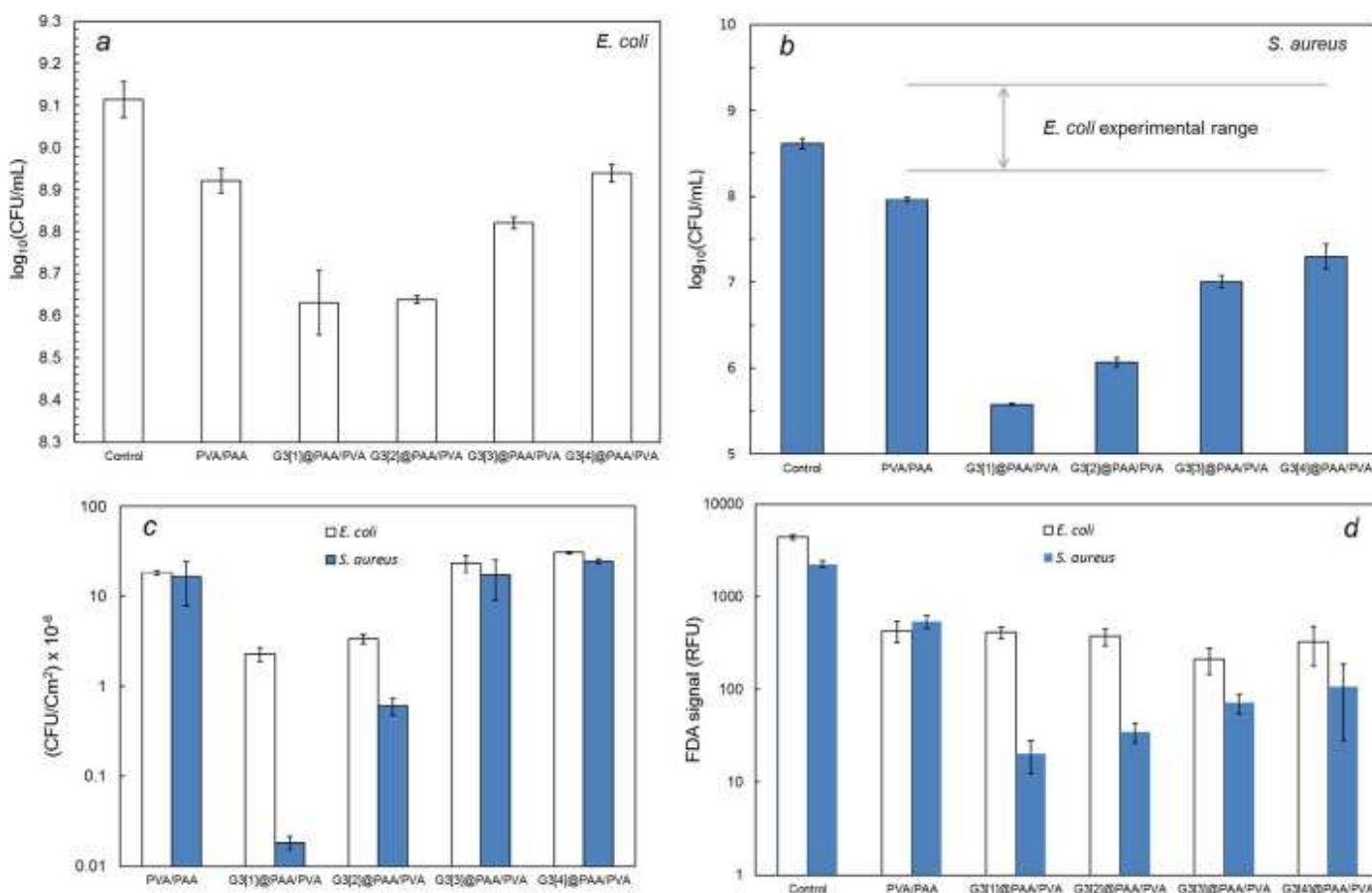


**Figure 3.** Colony-forming units (CFU) (a and b), viable microorganisms detached from membranes (c) and FDA metabolic signal (d). The bars identified as Control correspond to liquid cultures in the absence of membranes.

The effect of PAMAM dendrimers on microbial cells has been attributed to their positive charge, which is recognized to favor the interaction with the negatively charged biological membranes (Stasko et al., 2007). The interaction results in membrane disruption via nanohole formation (Nel et al., 2009). There are evidence of PAMAM dendrimer internalization in aquatic microorganisms that point towards their easy passage through cell membranes (Gonzalo et al., 2015). Although supported dendrimers are not expected to detach from PAA/PVA membranes and cause damage via internalization, membrane disruption upon contact interaction is the most probable cause of bacterial cell impairment. With respect to the culture without contact with membranes, the efficiency in avoiding new colonies was 99.9% for *S. aureus*. Again, the different cell structure could explain the different sensitivity of both strains to the antimicrobial action of dendrimer-loaded membranes. Further evidence supporting the antimicrobial effect of dendrimer-modified membranes is given in the series of SEM micrographs of Figs. S5 and S6 (SM). All SEM micrographs were taken after 20 h incubation at 36 °C of *E. coli* or *S. aureus* in contact with the different membranes prepared in this work. The results showed that G3[1]@PAA/PVA membranes were essentially free of *S. aureus* colonization, the effect being lower for membranes with less dendrimer. In all cases, the effect was lower for *E. coli* compared to *S. aureus* consistent with the other results reported here.

### 3.3. Removal of toluene from water

The results of toluene removal from aqueous solutions after equilibrium (12 h, 18 °C) are given in Fig. 4. For the lower concentrations, < 10 mg/L of toluene in the initial solution or < 2 µg toluene/mg membrane, the toluene removal was almost complete: > 95% for G3[1]@PAA/PVA and > 90% for PAA/PVA membranes.

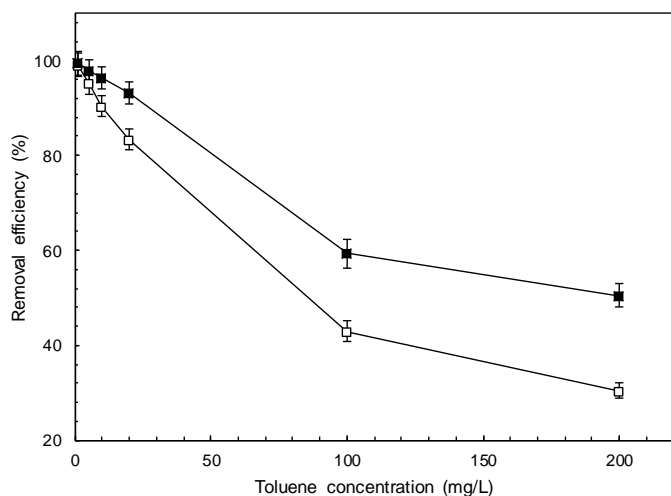


**Figure 4.** Toluene removal efficiency at different initial concentrations for PAA/PVA (□) and G3[1]@PAA/PVA (■) membranes.

The adsorption capacity for PAA/PVA and dendrimer-loaded membranes was related to the equilibrium concentration of toluene using the empirical Freundlich isotherm:

$$q = K_f c^{1/n} \quad (1)$$

where  $q$  is the equilibrium loading expressed in mg toluene/g of membrane,  $c$  the equilibrium concentration of toluene (µg/L) in water and  $K_f$  and  $n$  parameters that depend on the specific interaction between adsorbate and adsorbent. The linear form of Eq. (1) is represented together with the experimental values obtained in Fig. 5. The estimated model parameters were  $K_f = 0.12 \pm 0.02$  for PAA/PVA and  $0.16 \pm 0.01$  (units as indicated before) for G3[1]@PAA/PVA, whereas the corresponding  $n$  values were  $2.56 \pm 0.04$  and  $2.38 \pm 0.06$  respectively ( $1/n$  0.39 and 0.41). The relatively low value of  $1/n$  is indicative of a highly curved isotherm due to the saturation of the adsorption sites available for toluene.

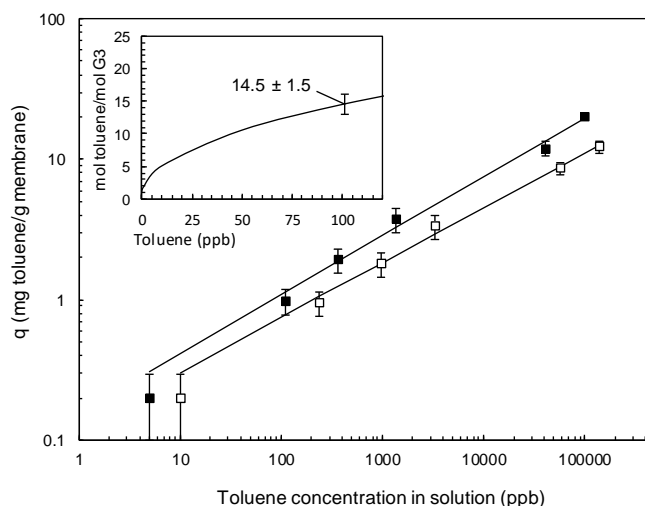


**Figure 5.** Toluene equilibrium loading as a function of the concentration of toluene in water for PAA/PVA (□) and G3[1]@PAA/PVA (■) membranes. Inset: amount of toluene adsorbed by G3 dendrimers in G3[1]@PAA/PVA membranes calculated from Freundlich fitting parameters.

The experimental results showed that PAA/PVA electrospun fibers retained a considerable amount of toluene (Fig. 5). PAA/PVA fibers are known to create a fabric network with very large surface-to-volume ratio and polar groups that favor the adsorption of polar pollutants (Santiago-Morales et al., 2016). The adsorption of the small dipole of toluene molecules (0.375 D) would be favored by polar carboxylic, hydroxyl and ester groups in PAA/PVA. There is evidence for attraction between the  $\pi$ -electrons of aromatic compounds and the hydrogen atoms of water in a hydrogen-bond like configuration with the aromatic ring acting as a hydrogen bond acceptor (Lopes et al., 2007). The toluene dissolution process, however, is endothermic with enthalpy of 0.41 kcal/mol at 298 K and the energetically preferred configuration is the  $\pi$ -

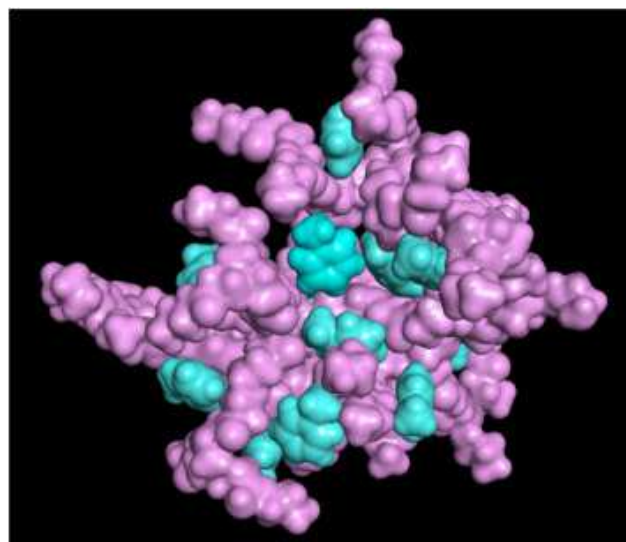
stacking interactions due to the strong interactions between adsorbed aromatic molecules. Intermolecular interactions have been shown to play an important role in toluene adsorption, with toluene molecules attracting each in an interaction that prevail over host–guest interactions (Szyja and Brodzik, 2007).

The results showed that toluene was retained in higher extension by membranes loaded with PAMAM G3 dendrimers. The amount of toluene adsorbed by the dendrimer can be calculated from the fitting values of the Freundlich isotherms and is given in the inset of Fig. 5. The value was 1.7 mol toluene/mol G3 for 1 mg/L of toluene in equilibrium and reached a  $14.5 \pm 1.5$  mol toluene/mol G3 for the highest concentrations used in this work. The interaction of toluene with the dendrimer molecules of functionalized fibers is studied in detail in the following section.

### 3.4. Docking calculations

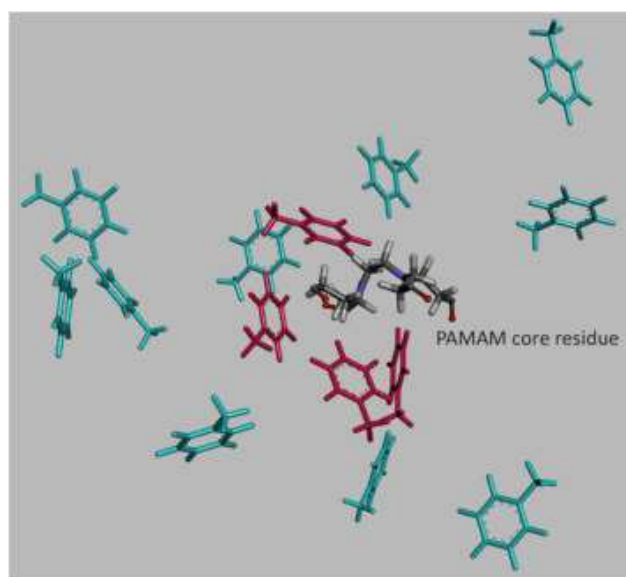
The interactions between adsorbates and dendrimers can be broadly divided into two categories: entrapment of drugs within the dendrimer architecture (generally involving electrostatic, hydrophobic and hydrogen bond interactions) and the interaction between drug and dendrimer surface (including electrostatic interactions and non-covalent bonding). The surface interactions between the adsorbate and dendrimer depend on the availability of specific surface groups on dendrimer surface. However, the encapsulation of substances within the dendrimer core structure occurs by a simple physical entrapment involving non-bonding interactions. The mode of binding depends on the structure and charge of the adsorbate as well as dendrimer features such as generation, core structure,  $pK_a$ , surface charge and the nature of its functional groups. PAMAM dendrimers, bearing a large number of cationic surface groups and internal amine groups, offer both surface binding and host-guest encapsulation. Due to their larger size, dendrimers of higher generations are capable of encapsulating higher amount of guest molecules inside compared to the lower generation ones, for which surface binding is often the preferred interaction with solutes.

Fig. 6 shows a snapshot of the association of toluene with PAMAM G3 dendrimer. The corresponding calculation showed that a maximum of 14 toluene molecules can be hosted inside the inner cavities of the dendrimer. The entrapment of toluene was favored by the hydrophobicity of the internal cavities of PAMAM dendrimers, which favor the hosting of small hydrophobic molecules such as toluene. The toluene molecules appeared in docking calculations in protected pocket-like structures formed between or under dendrimer branches. In all docking runs the estimated docking energy of the ligand was lower than  $-3$  kcal/mol.



**Figure 6.** Snapshot of toluene molecules (blue) associating to the PAMAM G3 dendrimer (pink).

One key factor in dendrimer-guest interactions is the location of the guest association sites within the dendrimer structure. At neutral pH conditions, the open structure of the PAMAM G3 dendrimer allowed four toluene molecules to diffuse to locations near the dendrimer center. The other ten molecules of toluene were located near the tertiary amines and between branches of the dendrimer. Fig. 7 displays their positions inside the PAMAM G3 molecule. The inset of Fig. 5 shows the number of toluene molecules per molecule of PAMAM G3 as a function of toluene concentration in solution. The capacity, excluding the toluene retained by the PAA/PVA fibers was calculated from the fitting parameters to Freundlich isotherms. The maximum experimental value was  $14.5 \pm 1.5$  mol toluene/mol PAMAM G3, in perfect agreement with the docking computations.



**Figure 7.** Toluene molecules associating to the PAMAM G3 dendrimer. Dendrimer center is shown in sticks and colored by element. Four toluene molecules colored in red near the center of the dendrimer. Ten toluene molecules colored in blue in the mid- and outer regions of the dendrimer.

#### 4. Conclusions

We prepared electrospun nanofibers from blends of poly(acrylic acid) and poly(vinyl alcohol). The fibers formed membranes stabilized via thermal crosslinking and functionalized by grafting amino-terminated PAMAM G3 dendrimers. The amino-terminated dendrimers were attached by inducing the formation of amide bonds with the carboxyl groups of poly(acrylic acid). The amount of dendrimer attached to fibers was in the 0.80–6.49  $\mu\text{mol}$  dendrimer/g membrane. After crosslinking, functionalization and water conditioning, the membranes displayed fiber swelling and occasional merging between adjacent fibers but preserved their fibrous morphology.

The antimicrobial activity of dendrimer-functionalized membranes was particularly high to the gram-positive bacterium *S. aureus* with a 99.9% reduction in its capacity of forming colonies adhered to the membrane. The effect was considerably lower for the gram-negative *E. coli* (< 90% for cell colonizing membrane surface). The decrease in cell metabolic activity was lower than the inhibition of the bacterial capacity to form new colonies, a result commonly due to the presence of viable but non-culturable bacteria. The effect of dendrimer-functionalized surface was attributed to the interaction of positively charged dendrimers with the negatively charged biological membranes.

PAMAM G3-functionalized membranes were tested for the removal of toluene from aqueous solutions. The results showed removal efficiencies > 95% for membranes containing 6.49  $\mu\text{mol}$  dendrimer/g membrane for initial concentrations of toluene < 10 mg/L (or < 2  $\mu\text{g}$  toluene/mg membrane and < 350  $\mu\text{g}$ /L in equilibrium). The docking simulations revealed that toluene-dendrimer association involved the cooperative formation of pocket-like structures between or under dendrimer branches. The calculations showed that the maximum number of toluene molecules hosted inside the inner cavities of the dendrimer was 14, in agreement with the maximum experimental value of  $14.5 \pm 1.5$  mol toluene/mol PAMAM G3.

#### Acknowledgements

Financial support for this work was provided by the FP7-ERA-Net Susfood, 2014/00153/001, the Ministry of Economy and Competitiveness, CTM2013-45775 and the Dirección General de Universidades e Investigación de la Comunidad de Madrid (S2013/MAE-2716). GA thanks the University of Alcalá for the award of pre-doctoral grants. The authors wish to thank Carmen García-Ruiz, from the Department of Analytical Chemistry of the University of Alcalá, for her help with ATR-FTIR measurements.

#### References

- Algarra M, Vázquez MI, Alonso B, Casado CM, Casado J, Benavente J. Characterization of an engineered cellulose based membrane by thiol dendrimer for heavy metals removal. *Chemical Engineering Journal* 2014; 253: 472-477.
- Altintas Z, Uludag Y, Gurbuz Y, Tohill I. Development of surface chemistry for surface plasmon resonance based sensors for the detection of proteins and DNA molecules. *Analytica Chimica Acta* 2012; 712: 138-144.
- Antonels NC, Benjamin Williams M, Meijboom R, Haumann M. Well-defined dendrimer encapsulated ruthenium SCILL catalysts for partial hydrogenation of toluene in liquid-phase. *Journal of Molecular Catalysis A: Chemical* 2016; 421: 156-160.
- Arndt KF, Richter A, Ludwig S, Zimmermann J, Kressler J, Kuckling D, et al. Poly(vinyl alcohol)/poly(acrylic acid) hydrogels: FT-IR spectroscopic characterization of crosslinking reaction and work at transition point. *Acta Polymerica* 1999; 50: 383-390.
- Astruc D, Boisselier E, Ornelas C. Dendrimers designed for functions: from physical, photophysical, and supramolecular properties to applications in sensing, catalysis, molecular electronics, photonics, and nanomedicine. *Chemical Reviews* 2010; 110: 1857-1959.
- Astruc D, Chardac F. Dendritic catalysts and dendrimers in catalysis. *Chemical Reviews* 2001; 101: 2991-3024.
- Bhattacharjee PK, Rutledge GC. Electrospinning and polymer nanofibers: Process fundamentals. *Comprehensive Biomaterials*. 1, 2011, pp. 497-512.
- Boas U, Heegaard PMH. Dendrimers in drug research. *Chemical Society Reviews* 2004; 33: 43-63.
- Boulos L, Prévost M, Barbeau B, Coallier J, Desjardins R. LIVE/DEAD® BacLight™: application of a new rapid staining method for direct enumeration of viable and total bacteria in drinking water. *Journal of Microbiological Methods* 1999; 37: 77-86.
- Brooks BR, Bruccoleri RE, Olafson BD, States DJ, Swaminathan S, Karplus M. CHARMM: A program for macromolecular energy, minimization, and dynamics calculations. *Journal of Computational Chemistry* 1983; 4: 187-217.
- Bukowska A, Bukowski W, Bester K, Flaga S. Linkage of the PAMAM type dendrimer with the gel type resin based on glycidyl methacrylate terpolymer as a method of preparation of the polymer support for the recyclable palladium catalyst for Suzuki-Miyaura cross-coupling reactions. *RSC Advances* 2015; 5: 49036-49044.
- Charles S, Vasanthan N, Kwon D, Sekosan G, Ghosh S. Surface modification of poly(amidoamine) (PAMAM) dendrimer as antimicrobial agents. *Tetrahedron Letters* 2012; 53: 6670-6675.
- Dubinsky S, Lumelsky Y, Grader GS, Shter GE, Silverstein MS. Thermal degradation of poly(acrylic acid) containing metal nitrates and the formation of  $\text{YBa}_2\text{Cu}_3\text{O}_{7-x}$ . *Journal of Polymer Science Part B: Polymer Physics* 2005; 43: 1168-1176.
- Gonzalo S, Rodea-Palomares I, Leganés F, García-Calvo E, Rosal R, Fernández-Piñas F. First evidences of PAMAM dendrimer internalization in microorganisms of environmental relevance: A linkage with toxicity and oxidative stress. *Nanotoxicology* 2015; 9: 706-718.

- Gratzl G, Walkner S, Hild S, Hassel AW, Weber HK, Paulik C. Mechanistic approaches on the antibacterial activity of poly(acrylic acid) copolymers. *Colloids and Surfaces B: Biointerfaces* 2015; 126: 98-105.
- Greiner A, Wendorff JH. Electrospinning: A fascinating method for the preparation of ultrathin fibers. *Angewandte Chemie - International Edition* 2007; 46: 5670-5703.
- Gross SA, Avens HJ, Banducci AM, Sahmel J, Panko JM, Tvermoes BE. Analysis of BTEX groundwater concentrations from surface spills associated with hydraulic fracturing operations. *Journal of the Air & Waste Management Association* 2013; 63: 424-432.
- Jin X, Hsieh YL. pH-responsive swelling behavior of poly(vinyl alcohol)/poly(acrylic acid) bi-component fibrous hydrogel membranes. *Polymer* 2005; 46: 5149-5160.
- Khin MM, Nair AS, Babu VJ, Murugan R, Ramakrishna S. A review on nanomaterials for environmental remediation. *Energy & Environmental Science* 2012; 5: 8075-8109.
- Kim B, Park H, Lee SH, Sigmund WM. Poly(acrylic acid) nanofibers by electrospinning. *Materials Letters* 2005; 59: 829-832.
- Kirwan LJ, Fawell PD, van Bronswijk W. In situ FTIR-ATR examination of poly(acrylic acid) adsorbed onto hematite at low pH. *Langmuir* 2003; 19: 5802-5807.
- Kumeta K, Nagashima I, Matsui S, Mizoguchi K. Crosslinking reaction of poly(vinyl alcohol) with poly(acrylic acid) (PAA) by heat treatment: Effect of neutralization of PAA. *Journal of Applied Polymer Science* 2003; 90: 2420-2427.
- Ledesma-García J, Escalante García IL, Rodríguez FJ, Chapman TW, Godínez LA. Immobilization of dendrimer-encapsulated platinum nanoparticles on pretreated carbon-fiber surfaces and their application for oxygen reduction. *Journal of Applied Electrochemistry* 2008; 38: 515-522.
- Lopes PEM, Lamoureux G, Roux B, MacKerell AD. Polarizable empirical force field for aromatic compounds based on the classical drude oscillator. *The Journal of Physical Chemistry. B* 2007; 111: 2873-2885.
- Maingi V, Jain V, Bharatam PV, Maiti PK. Dendrimer building toolkit: Model building and characterization of various dendrimer architectures. *Journal of Computational Chemistry* 2012; 33: 1997-2011.
- Malkoch M, Malmström E, Nyström AM. Dendrimers: Properties and Applications. *Polymer Science: A Comprehensive Reference*, 10 Volume Set. 6, 2012, pp. 113-176.
- Mansur HS, Oréface RL, Mansur AAP. Characterization of poly(vinyl alcohol)/poly(ethylene glycol) hydrogels and PVA-derived hybrids by small-angle X-ray scattering and FTIR spectroscopy. *Polymer* 2004; 45: 7193-7202.
- Montalbetti CAGN, Falque V. Amide bond formation and peptide coupling. *Tetrahedron* 2005; 61: 10827-10852.
- Morreale A, Maseras F, Iriepa I, Gálvez E. Ligand-receptor interaction at the neural nicotinic acetylcholine binding site: a theoretical model. *Journal of molecular graphics & modelling* 2002; 21: 111-118.
- Murugan E, Rangasamy R. Synthesis, characterization, and heterogeneous catalysis of polymer-supported poly(propyleneimine) dendrimer stabilized gold nanoparticle catalyst. *Journal of Polymer Science, Part A: Polymer Chemistry* 2010; 48: 2525-2532.
- Nel AE, Mädler L, Velegol D, Xia T, Hoek EMV, Somasundaran P, et al. Understanding biophysicochemical interactions at the nano-bio interface. *Nature Materials* 2009; 8: 543-557.
- Nouh SA, Bahareth RA. Effect of electron beam irradiation on the structural, thermal and optical properties of poly(vinyl alcohol) thin film. *Radiation Effects and Defects in Solids* 2013; 168: 274-285.
- Park JC, Ito T, Kim KO, Kim KW, Kim BS, Khil MS, et al. Electrospun poly(vinyl alcohol) nanofibers: effects of degree of hydrolysis and enhanced water stability. *Polymer Journal* 2010; 42: 273-276.
- Quirós J, Boltes K, Rosal R. Bioactive applications for electrospun fibers. *Polymer Reviews* 2016; 56: 631-667.
- Quiros J, Borges JP, Boltes K, Rodea-Palomares I, Rosal R. Antimicrobial electrospun silver-, copper- and zinc-doped polyvinylpyrrolidone nanofibers. *Journal of Hazardous Materials* 2015; 299: 298-305.
- Ramamurthy T, Ghosh A, Pazhani GP, Shinoda S. Current perspectives on viable but non-culturable (VBNC) pathogenic bacteria. *Frontiers in Public Health* 2014; 2: 103.
- Sanagi MM, Chong MH, Endud S, Ibrahim WAW, Ali I. Nano iron porphyrinated poly(amidoamine) dendrimer mobil composition matter-41 for extraction of N-nitrosodiphenylamine nitrosamine from water samples. *Microporous and Mesoporous Materials* 2015; 213: 68-77.
- Santiago-Morales J, Amariei G, Letón P, Rosal R. Antimicrobial activity of poly(vinyl alcohol)-poly(acrylic acid) electrospun nanofibers. *Colloids and Surfaces B: Biointerfaces* 2016; 146: 144-151.
- Satija J, Karunakaran B, Mukherji S. A dendrimer matrix for performance enhancement of evanescent wave absorption-based fiber-optic biosensors. *RSC Advances* 2014; 4: 15841-15848.
- Silhavy TJ, Kahne D, Walker S. The bacterial cell envelope. *Cold Spring Harbor Perspectives in Biology* 2010; 2: a000414.
- Stasko NA, Johnson CB, Schoenfisch MH, Johnson TA, Holmuhamedov EL. Cytotoxicity of polypropyleneimine dendrimer conjugates on cultured endothelial cells. *Biomacromolecules* 2007; 8: 3853-3859.
- Svenson S, Tomalia DA. Dendrimers in biomedical applications - Reflections on the field. *Advanced Drug Delivery Reviews* 2005; 57: 2106-2129.
- Szyja B, Brodzik K. Modeling the adsorption of aromatic compounds on the TiO<sub>2</sub>/SiO<sub>2</sub> catalyst. *Journal of Molecular Modeling* 2007; 13: 731-737.
- Thavasi V, Singh G, Ramakrishna S. Electrospun nanofibers in energy and environmental applications. *Energy & Environmental Science* 2008; 1: 205-221.
- Tomalia DA, Naylor AM, Goddard WA. Starburst dendrimers. Molecular-level control of size, shape, surface-chemistry, topology and flexibility from atoms to macroscopic matter. *Angewandte Chemie-International Edition in English* 1990; 29: 138-175.
- Trott O, Olson AJ. AutoDock Vina: Improving the speed and accuracy of docking with a new scoring function, efficient optimization, and multithreading. *Journal of Computational Chemistry* 2010; 31: 455-461.
- Tsubokawa N, Hosoya M, Kurumada J. Grafting reaction of surface carboxyl groups on carbon black with polymers having terminal hydroxyl or amino groups using N,N'-

- dicyclohexylcarbodiimide as a condensing agent. *Reactive & Functional Polymers* 1995; 27: 75-81.
- Valdés O, Vergara C, Nachtigall FM, Lopez-Cabaña Z, Tapia J, Santos LS. PAMAM built-on-silicon wafer thin-layer extraction devices for selective metal contamination detection. *Tetrahedron Letters* 2016; 57: 2468-2473.
- Valeur E, Bradley M. Amide bond formation: beyond the myth of coupling reagents. *Chemical Society Reviews* 2009; 38: 606-631.
- Vögtle F, Richardt G, Werner N. *Dendrimer Chemistry: Concepts, Syntheses, Properties, Applications*, 2009.
- WHO. *Guidelines for drinking-water quality*. Geneva: WHO Library Cataloguing-in-Publication Data, 2011.
- Zhang C, Yuan X, Wu L, Han Y, Sheng J. Study on morphology of electrospun poly(vinyl alcohol) mats. *European Polymer Journal* 2005; 41: 423-432.
- Zhang PM, Gao MX, Zhang XM. Functional dendrimer modified ultra-hydrophilic trapping copolymer network towards highly efficient cell capture. *Talanta* 2016; 153: 366-371.
- Zhao Y, Zhu X, Liu H, Luo Y, Wang S, Shen M, et al. Dendrimer-functionalized electrospun cellulose acetate nanofibers for targeted cancer cell capture applications. *Journal of Materials Chemistry B* 2014; 2: 7384-7393.

# SUPPLEMENTARY MATERIAL

## Dendrimer-functionalized electrospun nanofibres as dual-action water treatment membranes

Georgiana Amariei<sup>1</sup>, Javier Santiago-Morales<sup>1</sup>, Karina Boltes<sup>1</sup>, Pedro Letón<sup>1</sup>, Isabel Iriepa<sup>2</sup>, Ignacio Moraleda<sup>2</sup>, Amadeo R. Fernández-Alba<sup>3</sup>, Roberto Rosal<sup>1,\*</sup>

<sup>1</sup> Department of Chemical Engineering, University of Alcalá, E-28871 Alcalá de Henares, Madrid, Spain

<sup>2</sup> Department of Organic Chemistry and Inorganic Chemistry, School of Biology, Environmental Sciences and Chemistry, University of Alcalá, E-28871 Alcalá de Henares, Madrid, Spain

<sup>3</sup> Department of Analytical Chemistry, Agrifood Campus of International Excellence (ceiA3), European Union Reference Laboratory for Pesticide Residues in Fruit & Vegetables, University of Almería, E-04010 Almería, Spain

**Figure S1.** SEM micrographs of dendrimer-functionalized PAA/PVA membranes (nomenclature given in Table 1).

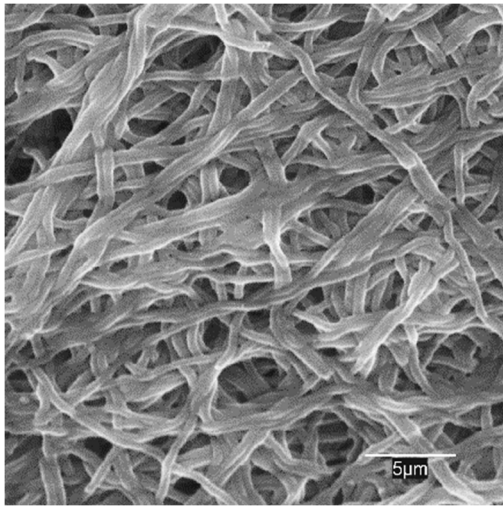
**Figure S2.** AFM image (a), height profile (b, along the line shown in a), AFM 3D image (c) and phase image (d) of a G3[1]@PAA/PVA membrane.

**Figure S3.** Live/Dead confocal micrographs of *E. coli* in liquid culture in contact with G3[1]@PAA/PVA and PAA/PVA membranes (a-d) and on membrane surface (e-h).

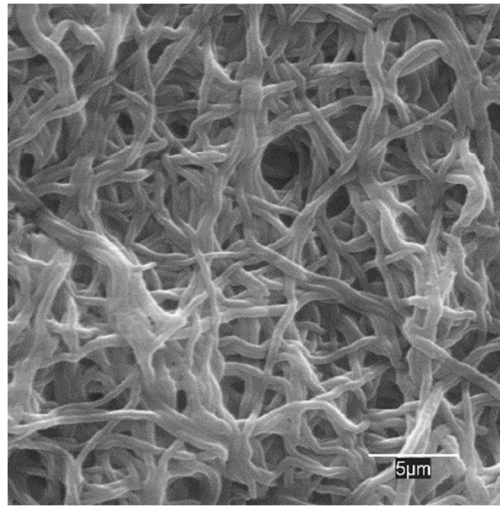
**Figure S4.** Live/Dead confocal micrographs of *S. aureus* in liquid culture in contact with G3[1]@PAA/PVA and PAA/PVA membranes (a-d) and on membrane surface (e-h).

**Figure S5.** SEM images of membranes in contact with *E. coli* cultures for 20 h at 36 °C.

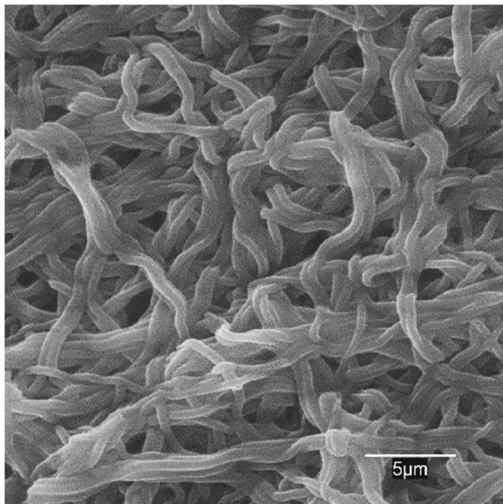
**Figure S6.** SEM images of membranes in contact with *S. aureus* cultures for 20 h at 36 °C.



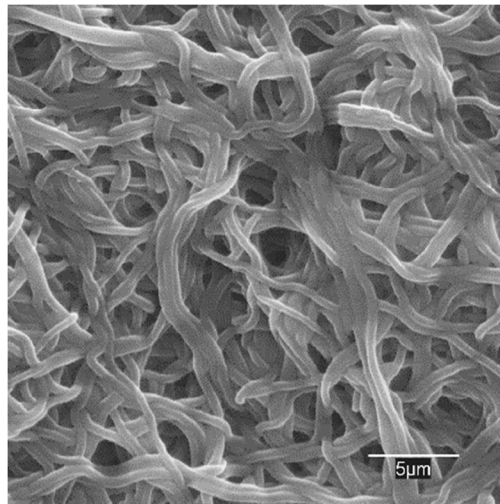
G3[1]@PAA/PVA



G3[2]@PAA/PVA



G3[3]@PAA/PVA



G3[4]@PAA/PVA

**Figure S1.** SEM micrographs of dendrimer-functionalized PAA/PVA membranes (nomenclature given in Table 1).

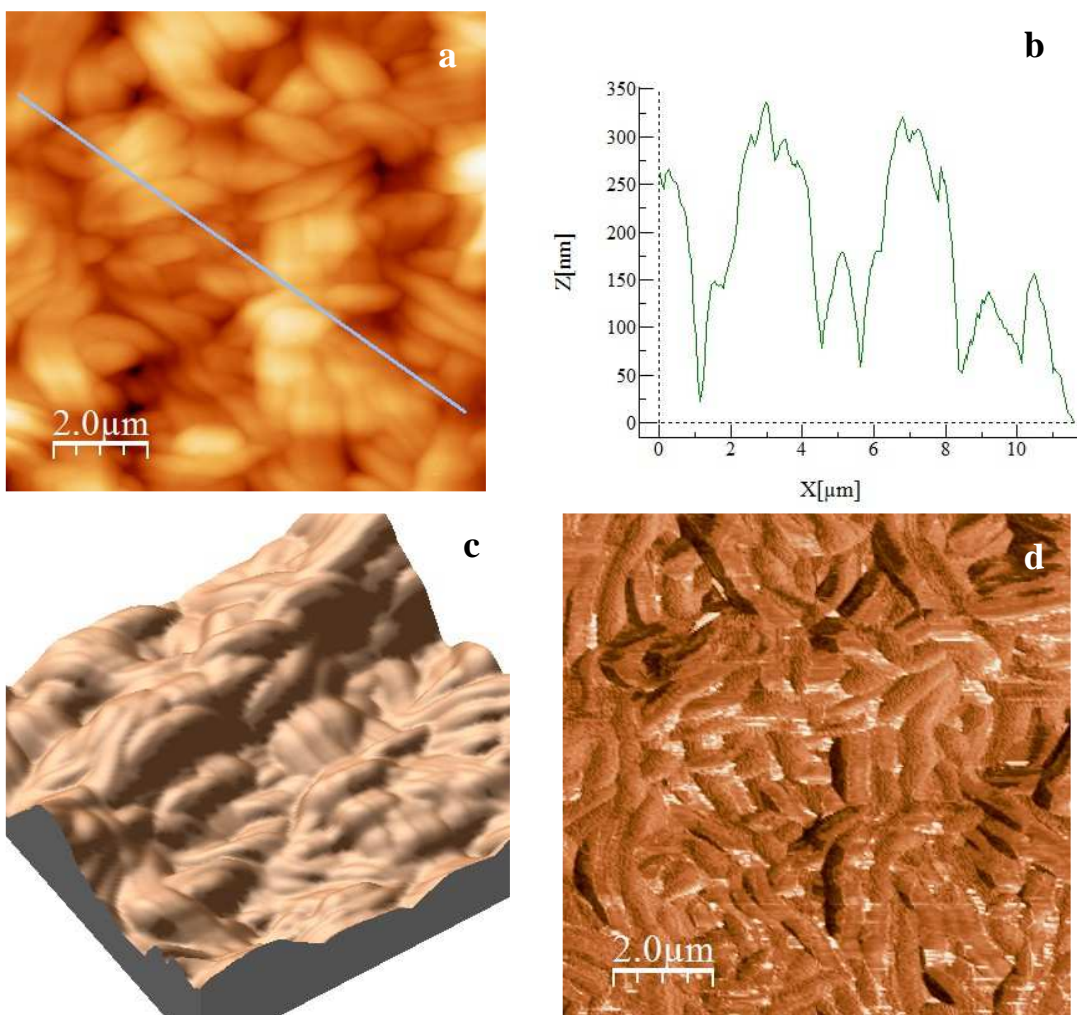


**Figure S2.** AFM image (a), height profile (b, along the line shown in a), AFM 3D image (c) and phase image (d) of a G3[1]@PAA/PVA membrane.

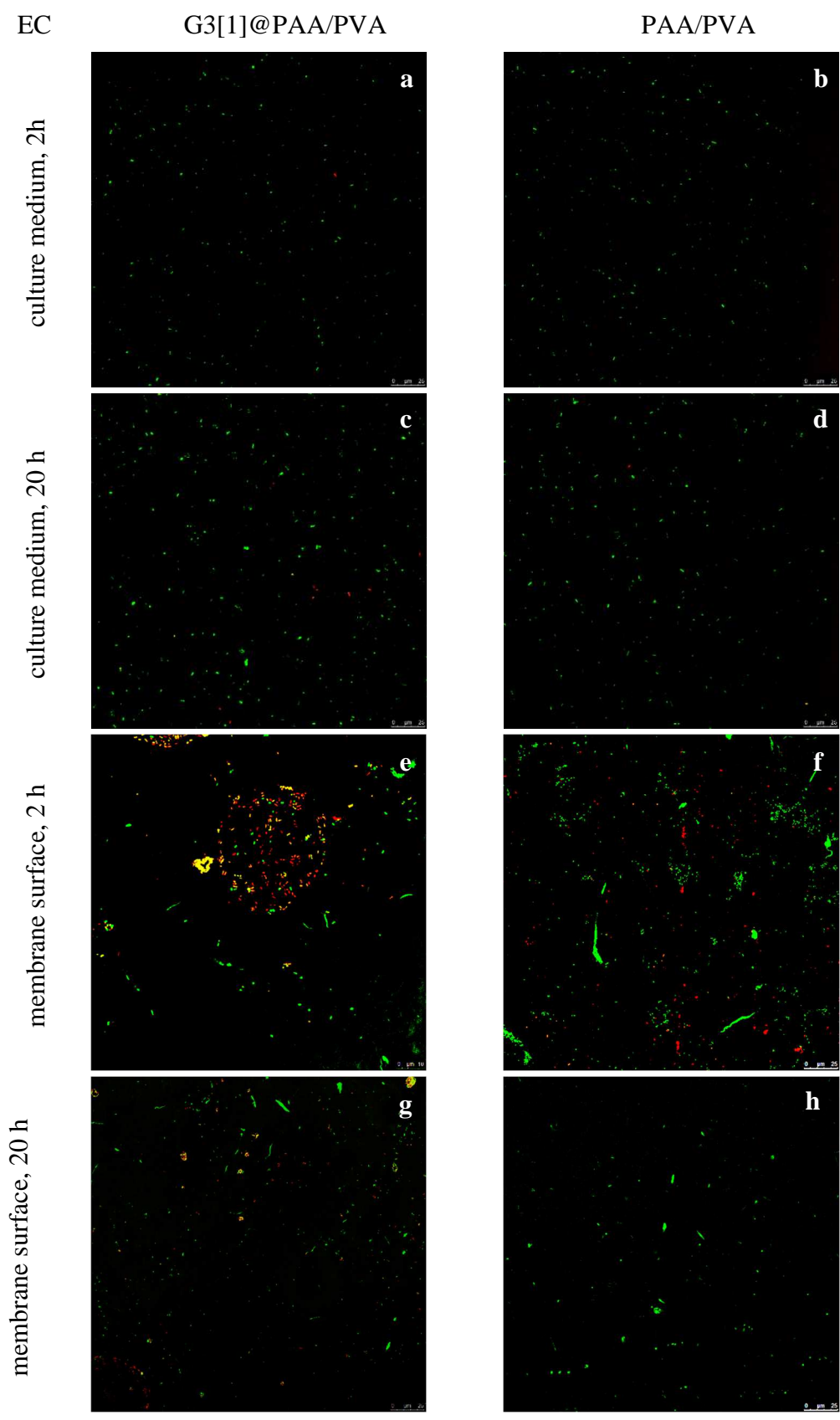


**Figure S3.** Live/Dead confocal micrographs of *E. coli* in liquid culture in contact with G3[1]@PAA/PVA and PAA/PVA membranes (a-d) and on membrane surface (e-h).

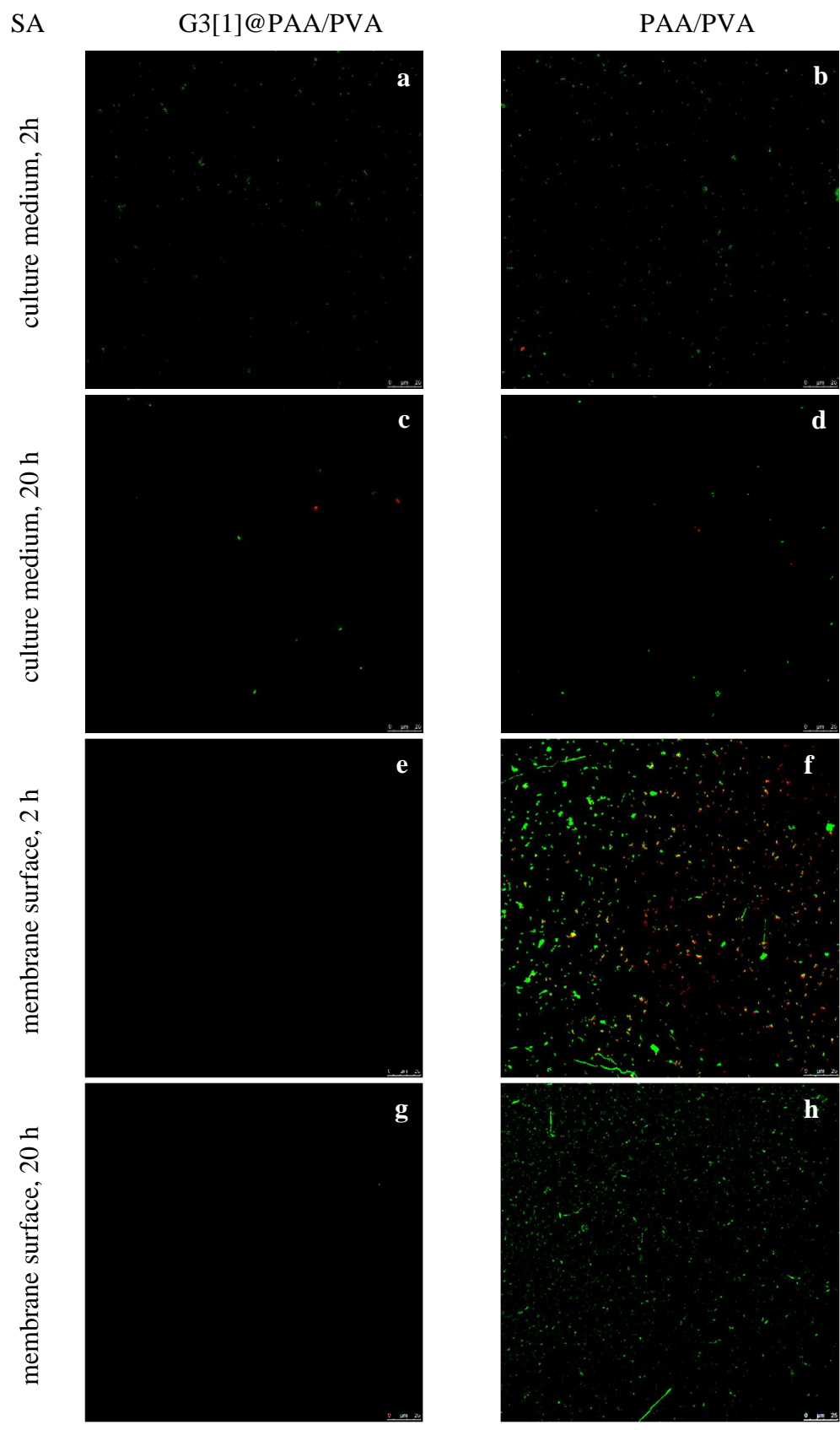
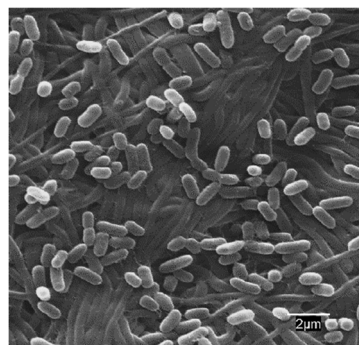
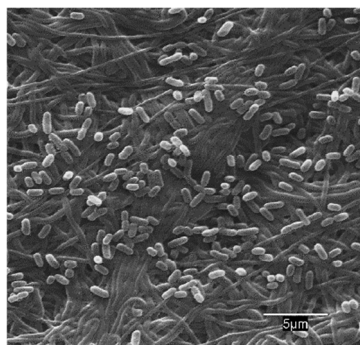
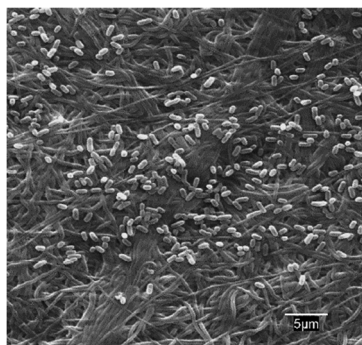
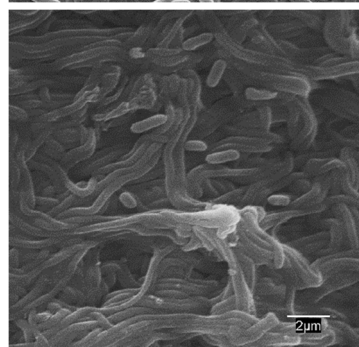
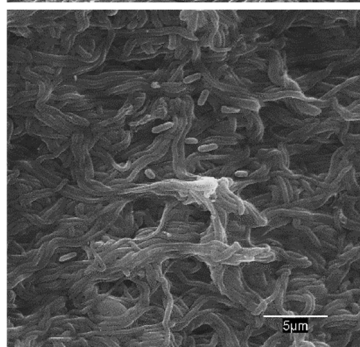
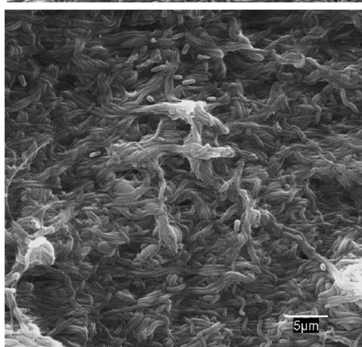


**Figure S4.** Live/Dead confocal micrographs of *S. aureus* in liquid culture in contact with G3[1]@PAA/PVA and PAA/PVA membranes (a-d) and on membrane surface (e-h).

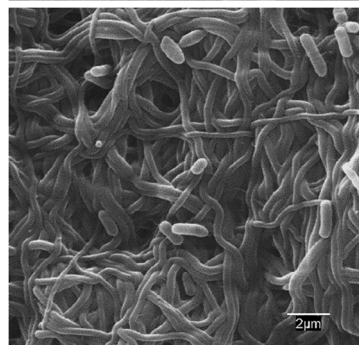
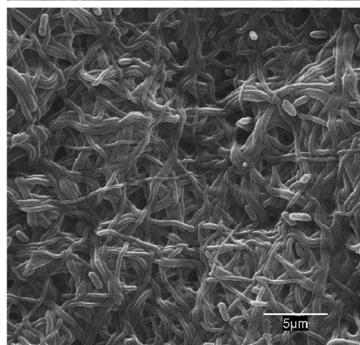
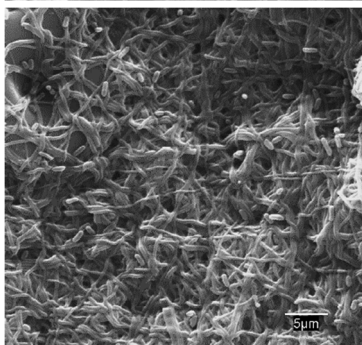
PAA/PVA



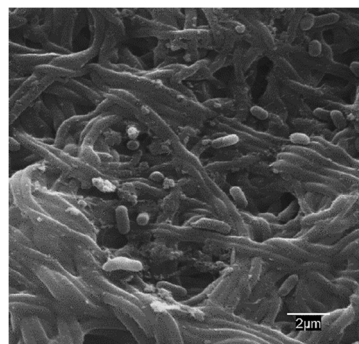
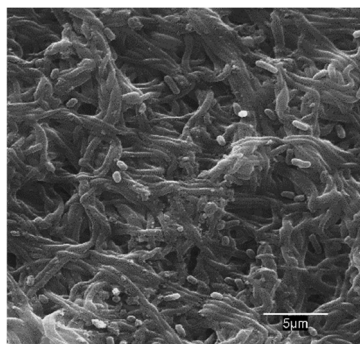
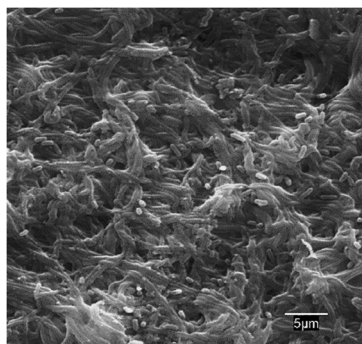
G3[1]@PAA/PVA



G3[2]@PAA/PVA



G3[3]@PAA/PVA



G3[4]@PAA/PVA

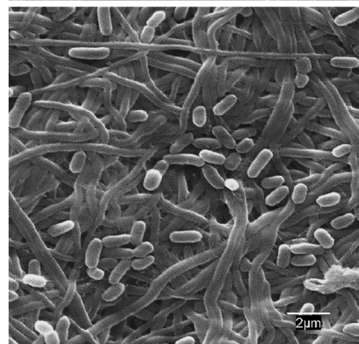
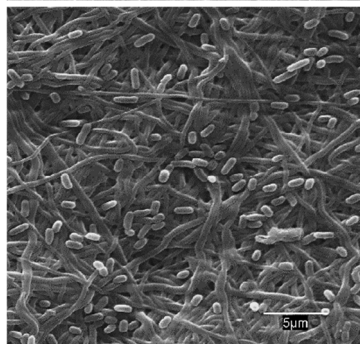
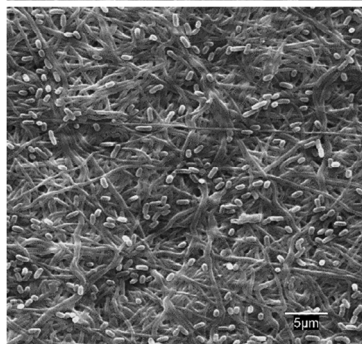
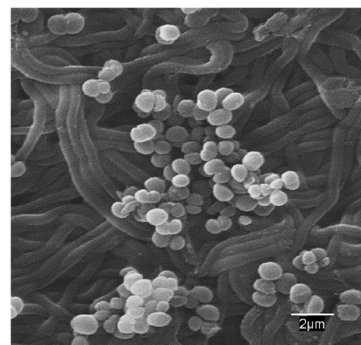
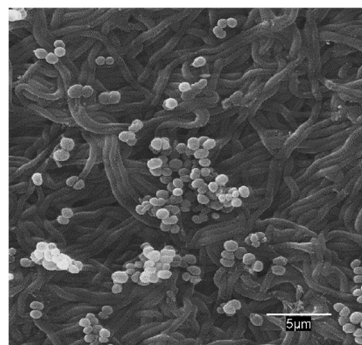
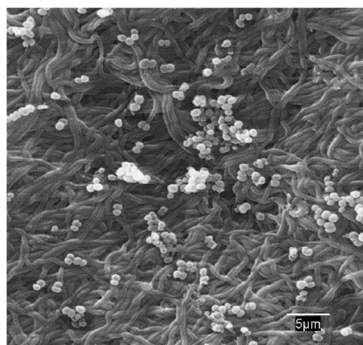
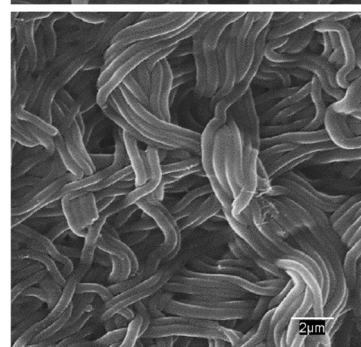
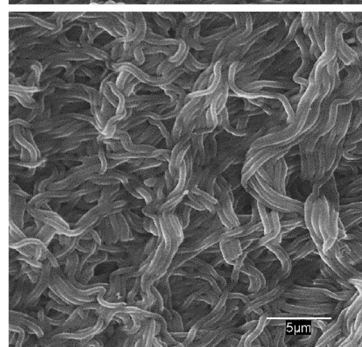
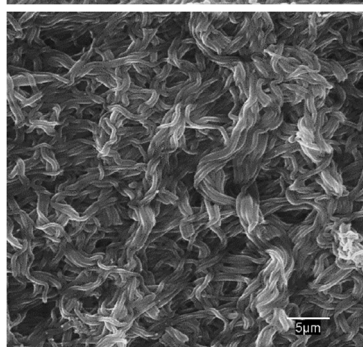


**Figure S5.** SEM images of membranes in contact with *E. coli* cultures for 20 h at 36 °C.

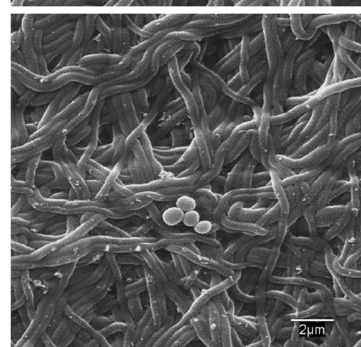
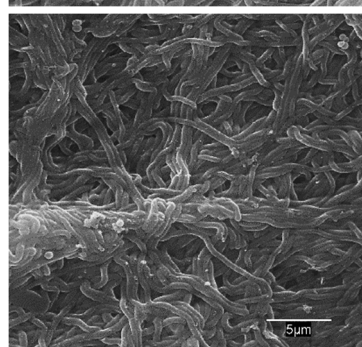
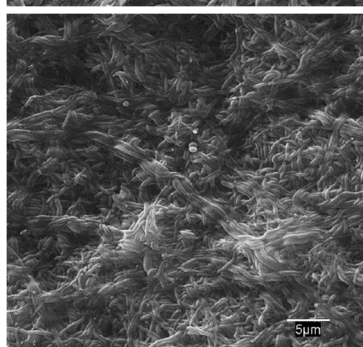
PAA/PVA



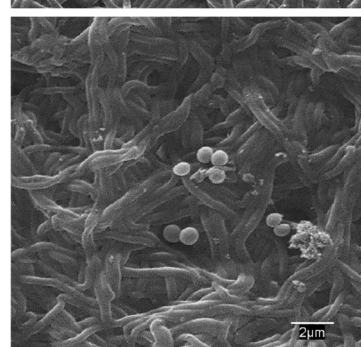
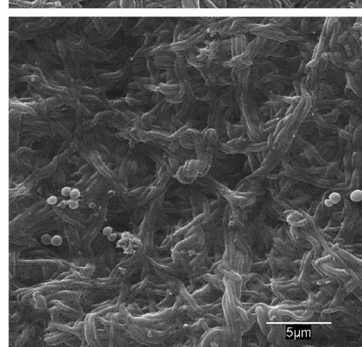
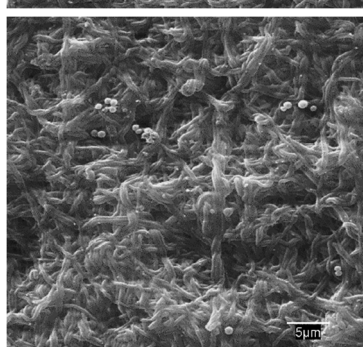
G3[1]@PAA/PVA



G3[2]@PAA/PVA



G3[3]@PAA/PVA



G3[4]@PAA/PVA

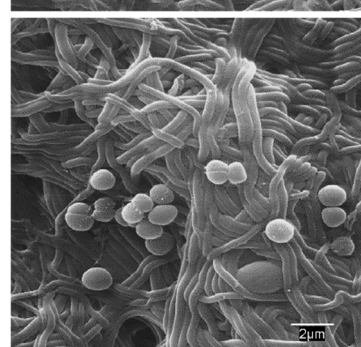
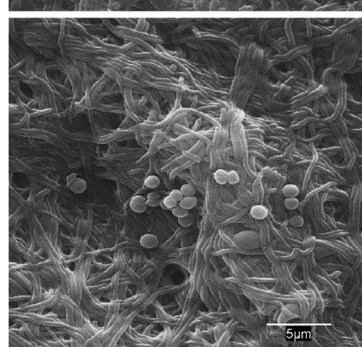
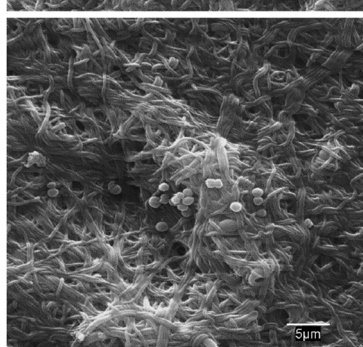


**Figure S6.** SEM images of membranes in contact with *S. aureus* cultures for 20 h at 36 °C.